Improved Accuracy of the Power Hardware-in-the-Loop Modeling using Multirate Discrete Domain

Fargah Ashrafidehkordi
Institute for Technical Physics
Karlsruhe Institute of Technology
Karlsruhe, Germany
0000-0003-1885-3573

Giovanni De Carne
Institute for Technical Physics
Karlsruhe Institute of Technology
Karlsruhe, Germany
0000-0002-3700-2902

2022 IEEE 13th International Symposium on Power Electronics for Distributed Generation Systems (PEDG) | 978-1-6654-6618-9/22/$31.00 ©2022 IEEE | DOI: 10.1109/PEDG54999.2022.9923128

***Abstract*—Power Hardware-in-the-Loop (PHIL) enables realistic hardware testing interfacing with a simulated environment. The PHIL nature calls for power interfaces, such as analog-to-digital converters, the power amplifier, and sensors, containing latency and noise. These elements are non-ideal, leading to inaccuracies and even instability. Accordingly, accurate modeling of a PHIL setup has become a challenging research topic. This paper presents accurate modeling of a PHIL setup approaching the actual hybrid analog/digital PHIL characteristics to ensure high accuracy in a wide frequency spectrum range. The proposed technique applies multirate discrete modeling, considering digital/analog sections as if in an actual setup. The accuracy is defined and evaluated over the frequency range of interests. The prominent voltage-type ideal transformer method (V-ITM) is employed as the interface algorithm. The proposed multirate discrete modeling is compared with purely continuous and singular discrete modeling approaches, considering all interface delays and dynamics while operating different hardware, namely, RL and RLC load. Frequency responses reveal a significant accuracy improvement in the proposed method. The step response similarly confirms the better performance of the proposed model in replicating the transients. The modeling methods are simulated using Simulink/MATLAB to confirm the validity of the proposed model.**

***Index Terms*—Power hardware in the loop simulation, PHIL accuracy, continuous, single-rate discrete, multirate discrete**

I. INTRODUCTION

The augmentation of leading-edge renewables based on power electronics (PE) converters in the electric networks are ever-increasing promptly. Power technologies such as smart transformers, photovoltaic resources, energy storage, and electric vehicles are indispensable in shifting to modern power networks [1]–[3]. The behavior of these novel actual power technologies must be realistically evaluated before the final implementation to the main grid to guarantee safe and stable operation. The Power Hardware-in-the-Loop (PHIL) concept has been introduced to avoid the hazard of field testing while not merely depending on simulation results [4], [5]. In a PHIL system, the Hardware under Test (HuT) is interfaced with a simulated network in a Digital Real-Time Simulator (DRTS) (Fig. 1a). In an actual setup, power interfaces such as power amplifier (PA), A/D, D/A converters, and sensors are essential to joint HuT to the DRTS (Fig. 1b). These power interfaces introduce noises and latencies to the system, originating inaccuracy and even instability. Several interface algorithms are defined to improve the stability and accuracy of PHIL [6]–[8]. The Ideal Transformer Method (ITM) is reputed as an accurate and straightforward interface algorithm [9], [10]. Besides selecting an appropriate interface algorithm, precise modeling of the PHIL system is essential to avoid inexact outcomes. A PHIL setup consists of a digital system, solving the equations in the discrete-time (DT) domain, and the HuT as an analog system, usually simulated as a continuous-time (CT) system. Although authors in [11] approximate the whole system in CT, it has been shown that the DT assumption is more accurate in imitating the transients since the discretization effects are well-captured as well as delays [12]. However, single-rate DT may fail to accurately mimic the existing analog (hardware) section. The idea of specifying a shorter sampling time for modeling

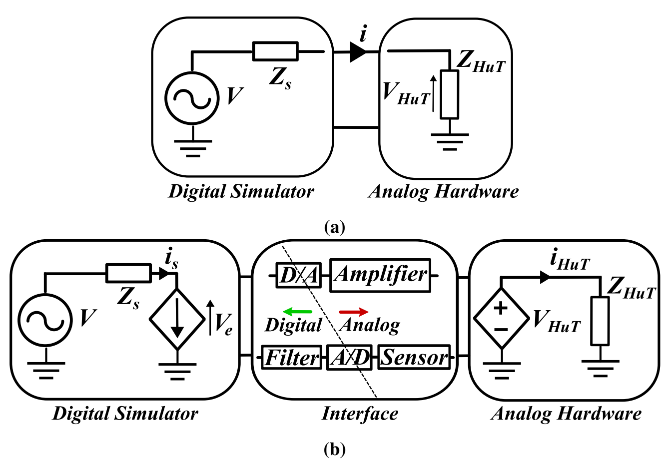

Fig. 1: Generic scheme of PHIL: (a) Ideal scheme, (b) Existing scheme with voltage-type ideal transformer method

This work was supported by the Helmholtz Association under the program "Energy System Design". The work of Giovanni De Carne was supported by the Helmholtz Association within the Helmholtz Young Investigator Group "Hybrid Networks" (VH-NG-1613).

the hardware part as a multirate discrete-time domain (MDT) model is examined in [13] to achieve stability enhancement; yet, the accuracy analysis of PHIL in a wide range frequency is overlooked.

This paper presents the MDT approach to model a PHIL setup with the voltage-type ideal transformer method (V-ITM), considering the dynamics and delays of power interfaces. A methodical definition of the accuracy based on the closed-loop transfer function is provided. The accuracy of three different modeling approaches, CT, DT, and MDT, is calculated and compared in the overall frequency spectrum. It is indicated that the MDT model leads to significantly more accurateness, particularly in phase than the complete CT and single-rate DT assumptions for both RL and RLC cases as HuT.

II. Definition of Accuracy

The accuracy of a PHIL model can be defined as the proximity of the models' gain and phase values to actual values at each frequency [14]. To better evaluate accuracy throughout the whole frequency spectrum, the mean error is selected and expressed as follows:

$$AVG_{gain} = \sum_{i=1}^{N} \frac{|G_{act}(j\omega)| - |G_{model}(j\omega)|}{|G_{act}(j\omega)|} \times 100 \quad (1)$$

$$AVG_{phase} = \sum_{i=1}^{N} \frac{\angle G_{act}(j\omega) - \angle G_{model}(j\omega)}{\angle G_{model}(j\omega)} \times 100 \quad (2)$$

Where $|G_{act}|$, and $\angle G_{act}$ are the gain and phase of the closed-loop system, chosen as a reference system and simulated in Simulink/MATLAB. $|G_{model}|$, and $\angle G_{model}$ implies the closed-loop transfer function of each CT, DT, and proposed MDT model of the V-ITM PHIL with the physical sense of grid admittance, seen by the HuT.

Considering that the majority of PHIL studies involve dynamics of relatively low frequency (e.g., below 2 kHz), the inverse of frequency in (1), (2) has been added to weight the error in the magnitude and phase. Hence, a weighted average error is defined as follows:

$$WAVG_{gain} = \sqrt{\sum_{i=1}^{N} \frac{|\frac{1}{f_i}(|G_{act}(j\omega)| - |G_{model}(j\omega)|)|^2}{|G_{act}(j\omega)|^2}} \times 100 \quad (3)$$

$$WAVG_{phase} = \sqrt{\sum_{i=1}^{N} \frac{|\frac{1}{f_i}(\angle G_{act}(j\omega) - \angle G_{model}(j\omega))|^2}{|\angle G_{act}(j\omega)|^2}} \times 100 \quad (4)$$

III. Modeling of V-ITM PHIL

Based on the definition of accuracy, this section focuses on obtaining the closed-loop transfer function of each CT, DT, and MDT modeling. The equivalent block diagram of each V-ITM PHIL modeling is shown in Fig. 2. Two different sampling times are chosen for the software and hardware sides of the PHIL in the MDT method. The primary time step (T_{s1}) is assigned to the software side of the PHIL, and the minor time step (T_{s2}), closer to the continuous-time domain, represents the hardware side. The discretization effects are well-captured. Thevenin model with an RL impedance is chosen as the simulated grid, and RL and RLC impedances are employed as HuT in two different scenarios. Delays of the A/D and D/A conversions, sensors, and DRTS are considered in addition to the PA and low-pass filter dynamics.

A. Continuous

According to Fig. 2a, the translated hardware current to the software environment $i_{s,HuT}$, over the input voltage v, defines the admittance of the whole setup and is chosen as the closed-loop transfer function of the system. The CT closed-loop transfer function is defined as:

$$G_{cl}(s) = G_{fw}(s)/(1 + G_{ol}(s)) \quad (5)$$
$$G_{ol}(s) = G_{fb}(s) \times G_{fw}(s) \quad (6)$$
$$G_{fb}(s) = G_{Filter}(s) \times G_s(s) \times e^{-(T_{d,DRTS})s} \quad (7)$$
$$G_{Filter}(s) = \omega_c/(s + \omega_c) \quad (8)$$
$$G_s(s) = L_s s + R_s \quad (9)$$
$$G_{fw}(s) = G_{PA}(s) \times G_{HuT}(s) \times e^{-(T_{d,fw})s} \quad (10)$$
$$G_{PA}(s) = \frac{a_1 s + b_1}{c_1 s^2 + d_1 s + e_1} \times e^{-(T_{d,Amp})s} \quad (11)$$
$$G_{HuT}(s) = 1/Z_{HuT}(s) \quad (12)$$
$$T_{d,fw} = T_{d,DRTS} + T_{d,D/A} + T_{d,Sens} + T_{d,A/D} \quad (13)$$

Where $G_{fw}(s)$ is the transfer function of the forward path from input to $i_{s,HuT}$, and $G_{ol}(s)$ is the open-loop transfer function. $T_{d,DRTS}$, $T_{d,D/A}$, $T_{d,A/D}$, $T_{d,Sensor}$, and $T_{d,Amp})s$ are delays introduced by DRTS, A/D and D/A conversions, sensor measurements, and power amplifier respectively. Parameters for the exclusive second-order transfer function of the switching-mode amplifier, $G_{PA}(s)$, are given in Table III, and ω_c is the cut-off frequency of the low-pass filter. The impedances of the hardware, $Z_{HuT}(s)$, for RL and RLC cases are:

$$\begin{aligned} Z_{HuT,RL}(s) &= R_{HuT} + L_{HuT}s \\ Z_{HuT,RLC}(s) &= Z_{HuT,RL}(s) + 1/(C_{HuT}s) \end{aligned} \quad (14)$$

B. Discrete

Respectively, Fig. 2b represents the discredited model of the same system. The Zero-Order Hold (ZOH) method is chosen to discretize the continuous $G_{cl}(s)$, where its transfer function is assumed as $(1 - e^{-(T_{s1})s})/s$. Applying it to the derived $G_{cl}(s)$ from section III-A and performing the z-transformation, the closed-loop DT transfer function of the system becomes:

$$\begin{aligned} G_{cl}(z) &= z\{(1 - e^{-(T_{s1})s})G_{cl}(s)/s\} \\ &= (1 - z^{-1})z\{G_{cl}(s)/s\} \end{aligned} \quad (15)$$

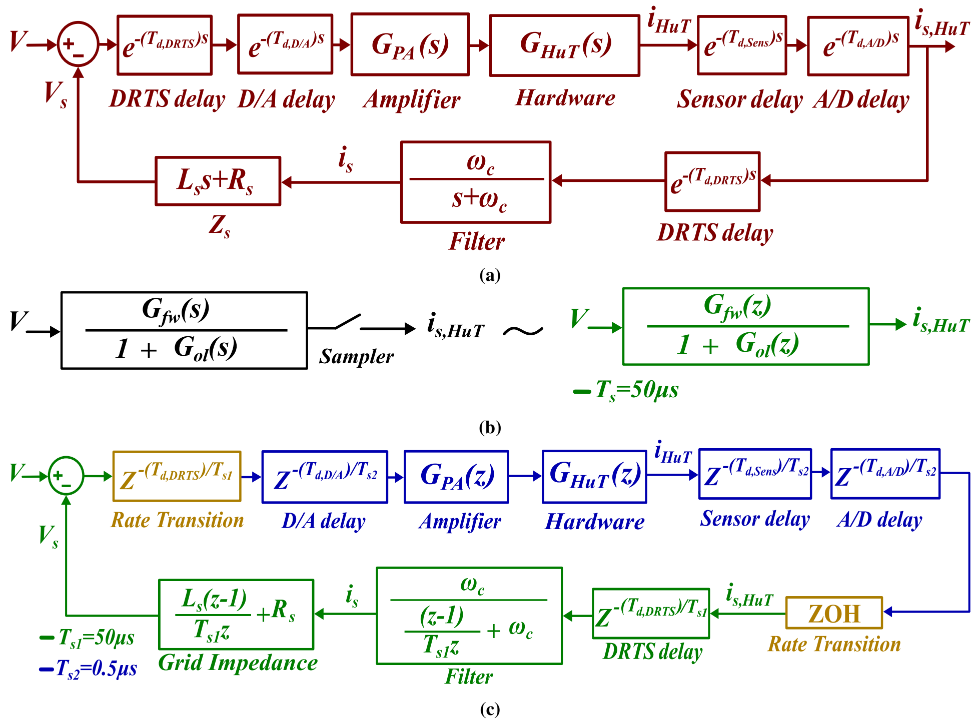

Fig. 2: Possible modeling block diagrams: (a) Continuous-time, (b) Discrete, (c) Multirate discrete

C. Multirate Discrete

The MDT model is a DT model with two different sampling times. The smaller sampling time, blue line in Fig. 2c, is assigned to the hardware model since it is relatively tight to the actual CT domain. Hence, CT parts, in reality, are represented here in DT equations but with a relatively shorter sampling time, $T_{s2} << T_{s1}$:

$$G_{cl}(z) = G_{fw}(z)/(1 + G_{ol})(z) \tag{16}$$

$$G_{PA}(z) = \frac{a_2 z + b_2}{c_2 z^2 + d_2 z + e_2} \times z^{-(T_{d,Amp}/T_{s2})} \tag{17}$$

$$G_{HuT}(z) = 1/Z_{HuT}(z) \tag{18}$$

$$Z_{HuT,RL}(z) = R_{HuT} + L_{HuT}(z-1)/(T_{s2}z) \tag{19}$$

$$Z_{HuT,RLC}(z) = Z_{HuT,RL}(z) + T_{s2}z/(C_{HuT}(z-1)) \tag{20}$$

Where $G_{fw}(z)$, and $G_{ol}(z)$ can be derived by following the same approach in section III-A, and III-B and using the given discrete transfer function of each component in Fig. 2c. Parameters of $G_{PA}(z)$ are given in Table III, illustrating affiliated discretized transfer function with the new sampling time.

IV. Simulation Results

With the closed-loop transfer function of the three models discussed above, the bode diagram is applied to attain a graphical understanding of accuracy comparisons in the frequency domain. The parameters for simulating the PHIL setup are given in Table IV. The gain and phase for each CT, DT, and MDT model are calculated and depicted in Fig. 3 and Fig. 6, respectively, when using RL and RLC load as HuT. The references of accuracy analysis (G_{act}), shown in red color, are the measured gain and phase at the frequency range from 50Hz to 4.5kHz using the Simulink/MATLAB. Accuracy calculation outcomes based on for RL and RLC load are elaborated as follows:

A. RL Load

As it is transparent in Fig. 3, and its zoomed plot on the frequency at 2.5 Hz, Fig. 4, the cyan color belonging to the MDT model is well-matched with the reference. As the frequency increases, phase deviations in the CT and DT model from the reference intensify, while the MDT sticks firmly to the reference throughout the spectrum. The accuracy is also calculated using (1) to (4), and compared in Table I, in line with the bode diagram outcomes. The DT method achieves the smallest AVG_{gain} error by 0.5%; however, AVG_{phase} reveals considerable error by 5.98%. The average MDT error is only about 0.2% more than DT in gain but around 5.9% lesser in phase. In other words, considering both gain and phase errors, achievements in MDT are triumphing. The $WAVG$ statistics of MDT display an error of less than 0.03% in gain and relatively negligible in phase, while CT and DT numbers stand above 0.1% and 0.4%, respectively, both in gain and phase. Furthermore, the step response shown in Fig. 5 depicts the MDT model replicates the transients better than the two others.

B. RLC Load

The MDT accuracy is examined under the resonance condition with an RLC load where the resonance frequency is 4kHz. While the overall performance in Fig. 6 may only demonstrate the higher-ranking of the MDT method in phase, a meticulous attention to the Fig. 7 reveals better execution of MDT for both gain and phase at the resonance frequency. Table I accredits the enhanced accurateness of MDT for the whole frequency spectrum. Indicators AVG_{gain} and $WAVG_{gain}$ are considerably improved from CT to DT model where error decreases from 3.7% to less than 1% in AVG_{gain} and by 0.01% in $WAVG_{gain}$, yet not more profitable than MDT. The artistic production of MDT can be seen according to AVG_{phase} and $WAVG_{phase}$, where the accuracy is improved by 7% and 0.05% compared with CT, though CT may be preferred over DT.

TABLE I: RL Accuracy Calculation

model / error(%)	MDT	CT	DT
AVG_{gain}	0.6976	3.2370	0.5083
AVG_{phase}	0.0678	4.2215	5.9873
$WAVG_{gain}$	0.0023	0.0143	0.0565
$WAVG_{phase}$	0.0004	0.0194	0.0458

TABLE II: RLC Accuracy Calculation

model / error(%)	MDT	CT	DT
AVG_{gain}	0.7850	3.7505	0.9250
AVG_{phase}	0.1088	7.0069	10.2232
$WAVG_{gain}$	0.0033	0.0138	0.0037
$WAVG_{phase}$	0.0008	0.0530	0.0765

TABLE III: PA transfer function coefficients

coefficients / index	a_i	b_i	c_i	d_i	e_i
$i = 1$	-263.1	1.836×10^5	1	234.5	1.841×10^5
$i = 2$	-1.315×10^{-4}	1.3160×10^{-4}	1	-2	0.9999

TABLE IV: PHIL simulation parameter

setup	T_{s_1}	T_{s_2}	$T_{d,DRTS}$	$T_{d,D/A}$	$T_{d,A/D}$	$T_{d,Sens}$
unit	$[\mu s]$	$[\mu s]$	$[\mu s]$	$[\mu s]$	$[\mu s]$	$[\mu s]$
value	50	0.5	50	3	3	3
setup	ω_c	L_s	L_{HuT}	C_{HuT}	R_s	R_{HuT}
unit	$[kHz]$	$[mH]$	$[mH]$	$[mF]$	$[\Omega]$	$[\Omega]$
value	2	0.4	4	0.4	0.06	0.6

V. Conclusion

The PHIL is a potent tool for testing energy technologies in a flexible low-risk environment. Despite the potential, non-idealities, noises, and inevitable delays arise from connecting the software and hardware parts of the experimental setup, and they demand accurate modeling to avoid inaccuracies. This paper examines the accuracy of a V-ITM PHIL by testing simple RL and RLC loads as HuT to compare the modeling with the simulation results. In addition to continuous-time and

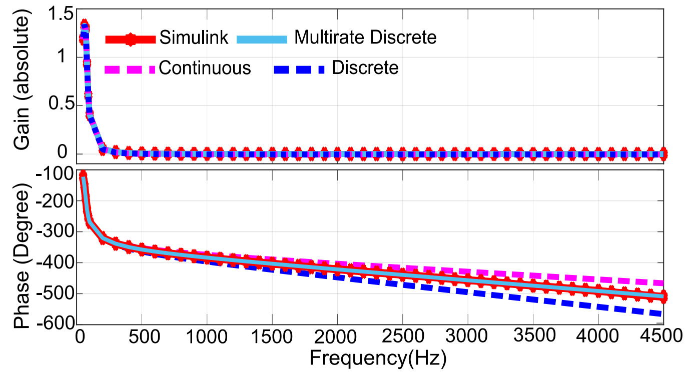

Fig. 3: Frequency response comparison using RL as HuT

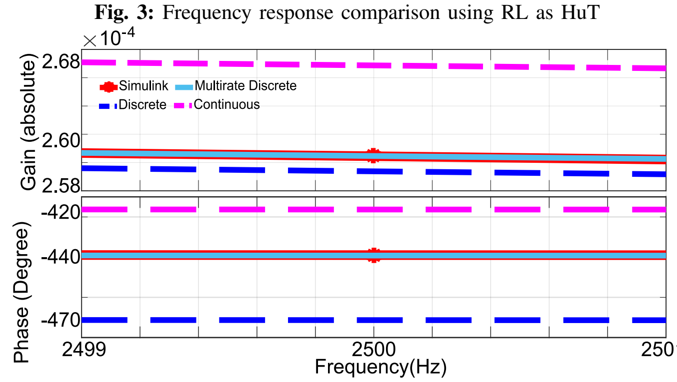

Fig. 4: Zoomed frequency response using RL at 2.5kHz

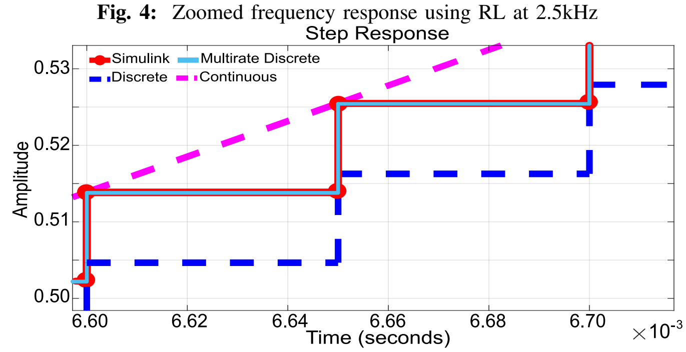

Fig. 5: Time-domain response RL as HuT

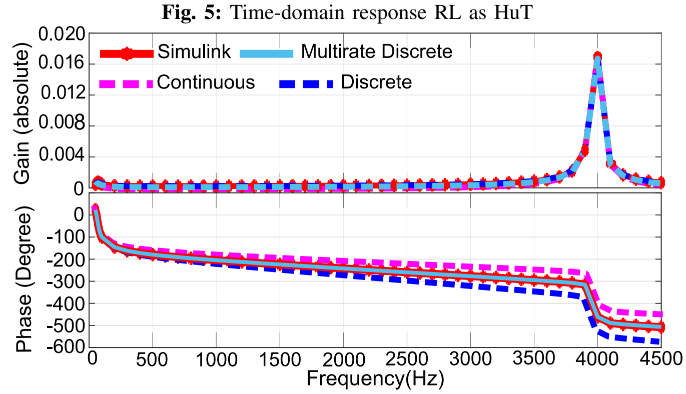

Fig. 6: Frequency response comparison using RLC as HuT

discrete modeling methods, which are classical approaches for this analysis, a multirate discrete method is proposed and compared in the [50Hz - 4.5kHz] frequency range concerning detailed Simulink/Matlab simulations. According to the Simulink output as a reference, gain and phase errors of three noted

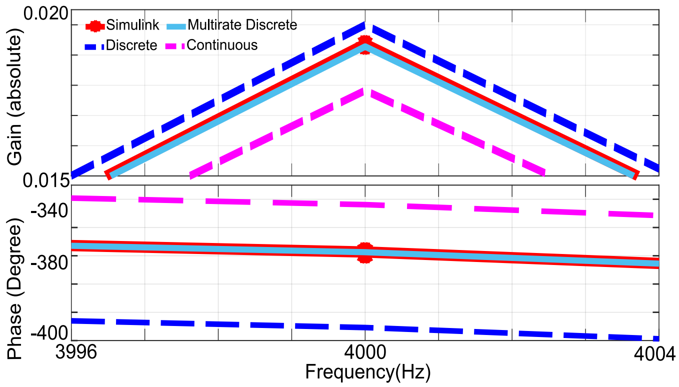

Fig. 7: Zoomed frequency response using RLC at 4kHz

modelings are calculated based on the admittance of HuT. Concerning the frequency of interest, the MDT method gives the smallest errors, outperforming the CT and DT modelings for both HuT cases. Furthermore, the step response ensures the high accuracy of the proposed MDT model, enabling a better replica of the transients.

REFERENCES

[1] S. Pugliese, M. Liserre and G. D. Carne, "Enhanced Current-Type P-HIL Interface Algorithm for Smart Transformers Testing," 2021 IEEE Energy Conversion Congress and Exposition (ECCE), 2021, pp. 1171-1178.

[2] S. Karrari, N. Ludwig, G. De Carne and M. Noe, "Sizing of Hybrid Energy Storage Systems using Recurring Daily Patterns," in IEEE Transactions on Smart Grid, 2022, pp. 1-1.

[3] Zou, Zhi-Xiang and Liu, Xingqi and Tang, Jian and De Carne, Giovanni and Liserre, Marco and Wang, Zheng and Cheng, Ming, "Power synchronization of smart transformers allowing universal operation in radial and meshed grids," CSEE Journal of Power and Energy Systems, 2022, pp. 1-9.

[4] I. Jayawardana, C. N. M. Ho and Y. Zhang, "A Comprehensive Study and Validation of a Power-HIL Testbed for Evaluating Grid-Connected EV Chargers," in IEEE Journal of Emerging and Selected Topics in Power Electronics, vol. 10, no. 2, pp. 2395-2410, April 2022.

[5] W. Li, G. Joos and J. Belanger, "Real-Time Simulation of a Wind Turbine Generator Coupled With a Battery Supercapacitor Energy Storage System," in IEEE Transactions on Industrial Electronics, vol. 57, no. 4, pp. 1137-1145, April 2010.

[6] J. Siegers and E. Santi, "Improved power hardware-in-the-loop interface algorithm using wideband system identification," 2014 IEEE Applied Power Electronics Conference and Exposition - APEC 2014, 2014, pp. 1198-1204.

[7] S. Paran and C. S. Edrington, "Improved power hardware in the loop interface methods via impedance matching," 2013 IEEE Electric Ship Technologies Symposium (ESTS), 2013, pp. 342-346.

[8] B. Lundstrom and M. V. Salapaka, "Optimal Power Hardware-in-the-Loop Interfacing: Applying Modern Control for Design and Verification of High-Accuracy Interfaces," in IEEE Transactions on Industrial Electronics, vol. 68, no. 11, pp. 10388-10399, Nov. 2021.

[9] Ren, W. and Steurer, M. and Baldwin, T. L., "Improve the Stability and the Accuracy of Power Hardware-in-the-Loop Simulation by Selecting Appropriate Interface Algorithms," 2007 IEEE/IAS Industrial Commercial Power Systems Technical Conference, 2007, pp. 1-7.

[10] M. Bokal, I. Papič and B. Blažič, "Stabilization of Hardware-in-the-Loop Ideal Transformer Model Interfacing Algorithm by Using Spectrum Assignment," in IEEE Transactions on Power Delivery, vol. 34, no. 5, pp. 1865-1873, Oct. 2019

[11] Dargahi, Mahdi and Ghosh, Arindam and Ledwich, Gerard, "Stability synthesis of power hardware-in-the-loop (PHIL) simulation," 2014 IEEE PES General Meeting — Conference Exposition, 2014, pp. 1-5.

[12] Upamanyu, Kapil and Narayanan, G., "Improved Accuracy, Modeling, and Stability Analysis of Power-Hardware-in-Loop Simulation With Open-Loop Inverter as Power Amplifier," IEEE Transactions on Industrial Electronics, vol. 67, 2020, pp. 369-378.

[13] Lauss, Georg and Strunz, Kai, "Multirate Partitioning Interface for Enhanced Stability of Power Hardware-in-the-Loop Real-Time Simulation," IEEE Transactions on Industrial Electronics, vol. 66, 2019, pp. 595–605.

[14] Lauss, Georg and Strunz, Kai, "Accurate and Stable Hardware-in-the-Loop (HIL) Real-Time Simulation of Integrated Power Electronics and Power Systems," IEEE Transactions on Power Electronics, vol. 36, 2021, pp. 10920-10932.